

---

# Residual Attention Net for Superior Cross-Domain Time Sequence Modeling

---

**Seth H. Huang**  
AARC  
Huawei Technologies  
seth.huang@huawei.com

**Xu Lingjie**  
AARC  
Huawei Technologies  
xulingjie2@huawei.com

**Jiang Congwei**  
AARC  
Huawei Technologies  
jiangcongwei1@huawei.com

## Abstract

We present a novel architecture, residual attention net (RAN), which merges a sequence architecture, *universal transformer*, and a computer vision architecture, *residual net*, with a high-way architecture for cross-domain sequence modeling. The architecture aims at addressing the long dependency issue often faced by recurrent-neural-net-based structures. This paper serves as a proof-of-concept for a new architecture, with RAN aiming at providing the model a higher level understanding of sequence patterns. To our best knowledge, we are the first to propose such an architecture. Out of the standard 85 UCR data sets, we have achieved 35 state-of-the-art results with 10 results matching current state-of-the-art results without further model fine-tuning. The results indicate that such architecture is promising in complex, long-sequence modeling and may have vast, cross-domain applications.

## 1 Introduction

Sequence modeling and time series modeling have been critical in real life applications. Their vast applications range from market demand forecast, missile defense, weather forecast, logistics calculation, shipping routes and cost prediction to even the spreading speed of contagions. However, there have been relatively few papers addressing sequence modeling in the artificial intelligence field, currently dominated by deep learning methodologies. There is also a surging interest in the investment field to incorporate deep learning methodologies to compete in ever-competitive financial markets [12]. However, there are three main challenges facing this type of data.

First, real life data may have long-dependency issues. The most popular sequence modeling methodology in artificial intelligence has been long-short-term memory (LSTM), which is a type of recurrent neural network. Second, financial data notoriously has high noise-to-signal ratio, which means the random information to actual pattern information can be quite imbalanced, and despite the modeling power of deep neural networks, the model learns primarily noises. It overfits easily and cannot generalize well [12].

Lastly, sequence data can often be non-stationary. This means that the patterns often change, and what the model learns may not be applicable to the new market scenarios. One way to compensate for this is to extend the look-back period to incorporate for historical data in the past so the model can recognize more pattern types [20]. This is also related to the first challenge as few models can

address the long-dependency issues - though LSTM was first created to tackle this challenge, it has not been able to solve this issue effectively and has since been replaced by other attention-based algorithms especially in the natural-language domain [15].

For sequence modeling tasks with deep learning, natural-language processing (NLP) has been at the forefront of innovations. For speech recognition and translation domains, many types of new architectures employing attention mechanism have been created such as attention-LSTM [13], transformer [7](bert), and Bert [5].

[1] has shown that attention mechanism has been much more effective than LSTM in language tasks, and this idea was recently adopted by [18] to tackle sequence classification tasks. Compared to other modeling techniques, the authors claim attention-based methodologies are better at addressing long-dependency issues [3].

Additionally, some researchers have adopted techniques from the computer vision field and transfer the architectures to sequence modeling. For example, [2] uses convolution neural net for sequence modeling. [16]. Recently in the statistics field, [8] uses residual neural net (ResNet) for sequence modeling and outperforms many benchmarks based on statistical method. Some newly developed statistical methods such as Hive and Hive-Cote have shown to be extremely powerful in some sequence modeling [6], but they are ensemble methods based on numerous previous models, and they take extremely long time to train [17] and are not practical for real-life applications [17]. The limitations call for a sophisticated model architecture which can be readily applied in a practical setting while alleviating the above three challenges.

Typically, it is in theory inappropriate to use convolution-based methodology to tackle sequence modeling. Though it does not have long-dependency issues [14] as the data points are not passed through to the next block but are output directly in the pooling layer (average or global), convolution-based methodologies are "translation-invariant," which simply means time and sequence are not captured in CNN-based models - the architecture does not care where the pattern is and only cares that it appears in the sequence [21]. This is in theory inappropriate for time-driven sequence modeling especially for noisy data.

A recent series of papers [9, 10, 11] focusing on LSTM-FCN, which combines LSTM and fully convolutional net (check proper name) and achieved numerous state-of-the-art (SOTA) results on public benchmarks. This paper series will feature prominently in our paper and has inspired our work here.

LSTM-FCN architecture focuses on two branches, once based on LSTM (and a variant attention-LSTM, an LSTM with attention block), and the other based on a simple, three-block convolutions. For a recent analysis [9], in what they call an "ablation test," they present the data represented in the CNN filters. The intriguing part for us is that, based on the visual examination, the filters, depending on the data sets, sometimes have a smoothing effect and other times making the sequence noisier while retaining the overall sequence structure. Though not the focus of this paper, a hypothesis is that, while the sequence model is able to capture the time aspect of the data, the CNN architecture through the filters can make the models more resistant to noises.

Our work here elaborates on this concept and attempts to address the three main issues facing sequence modeling by combining a transformer architecture [19] and a residual, high-way architecture [22] and examine the effectiveness with UCR's 85 public, sequence classification tasks.

## 2 Related Works

### 2.1 ResNet

Residual Networks called ResNet use residuals to reconstruct the mapping of the network. That is to say, the input  $x$  is introduced again to the result, so that the weight of the stacked layer tends to zero.

$$y = \mathcal{F}(x, \{W_i\}) + x \quad (1)$$

Here  $x$  and  $y$  are the input and output vectors of the layers considered. The function  $\mathcal{F}(x, \{W_i\})$  is the residual mapping to be learned.

In order to match the dimension of  $\mathcal{F}(x, \{W_i\})$  and  $x$ , add a linear projection  $W_s$  to the above equation as:

$$y = \mathcal{F}(x, \{W_i\}) + W_s x \quad (2)$$

## 2.2 Universal Transformer

The Universal Transformer, which is based on encoder-decoder architecture, has been proposed by [4]. The details of this architecture is briefly shown as follows.

**Encoder:** At first, for an input sequence with length  $m$ , initialize a matrix  $H^0 \in \mathbb{R}^{m \times d}$ , and each row of it is a  $d$ -dimensional embedding of the symbols at each position of the sequence. Then use the multi-headed dot-product self-attention mechanism to compute representations  $H^t$  at step  $t$ , followed by a recurrent transition function. In addition, output and layer normalization are also added as the residual connections.

Use the scaled dot-product attention which combines queries  $Q$ , keys  $K$  and values  $V$  as follows

$$ATTENTION(Q, K, V) = SOFTMAX\left(\frac{QK^T}{\sqrt{d}}\right)V \quad (3)$$

$d$  is the number of columns of  $Q$ ,  $K$  and  $V$ . Then based on this equation, use the multi-head version with  $k$  heads.

$$MULTIHEADSELFATTENTION(H^t) = CONCAT(head_1, \dots, head_k)W^O \quad (4)$$

where

$$head_1 = ATTENTION(H^t W_i^Q, H^t W_i^K, H^t W_i^V) \quad (5)$$

and  $W^Q, W^K, W^V, W^O \in \mathbb{R}^{d \times d/k}$ .

So the revised representations  $H^t \in \mathbb{R}^{m \times d}$  are computed as follows

$$H^t = LAYERNORM(A^t + TRANSITION(A^t)) \quad (6)$$

where

$$A^t = LAYERNORM((H^{t-1} + P^t) + MULTIHEADSELFATTENTION(H^{t-1} + P^t)) \quad (7)$$

$P^t \in \mathbb{R}^{m \times d}$  are fixed, constant, two-dimensional (position, time) coordinate embeddings, for the positions  $1 \leq i \leq m$  and the time-step  $1 \leq t \leq T$  separately for each vector-dimension  $1 \leq j \leq d$ ,

$$P_{i,2j}^t = \sin i/10000^{2j/d} + \sin t/10000^{2j/d} \quad (8)$$

$$P_{i,2j+1}^t = \cos i/10000^{2j/d} + \cos t/10000^{2j/d}. \quad (9)$$

Finally, the output of encoder is a matrix of  $d$ -dimensional vector representation  $H^T \in \mathbb{R}^{m \times d}$  for the  $m$  symbols of the input sequence after  $T$  steps[4].

**Decoder:** The structure of the decoder is the same as the encoder. Specifically, after the self-attention function, the decoder also attends to the final encoder representation  $H^T$  of each position in input sequence using the Equation(2). But the queries  $Q$  obtained from projecting the decoder representation, and keys and values obtained from projecting the encoder representation[4]. During training, the decoder input is the target output, and finally, per-symbol target distributes are obtained:

$$P(y_{pos}|y_{[1:pos-1]}, H^T) = SOFTMAX(OH^T) \quad (10)$$

where  $O \in \mathbb{R}^d \times V$  is an affine transformation from the final decoder state to the output vocabulary size  $V$ . Softmax yields an  $(m \times V)$ -dimension output matrix normalized over its rows. Then select the maximal probability symbol as the next symbol.

Figure1 is just the architecture of the combination of ResNet and Universal Transformer.

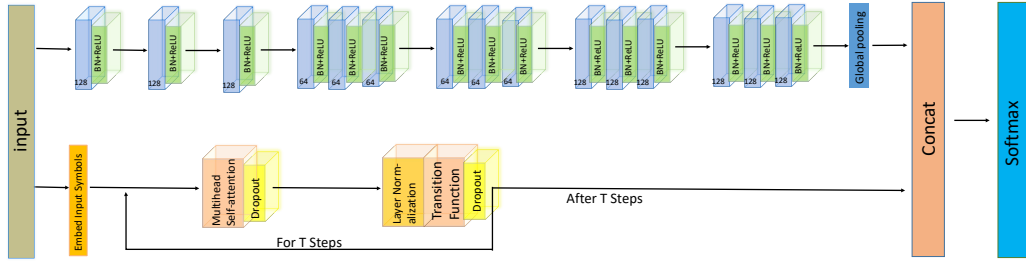


Figure 1: Resnet-Transformer architecture

### 3 Experimental Results

Here, we present the experimental results between previously existing SOTAs, the LSTM-FCN results (in some cases exceeding the SOTAs) and the Resnet-Transformer results. For LSTM-FCN, we reproduced experimental results and took the best results among several training cycles, following the approach in [9]. Notice that, the reported results in [9] are fine-tuned for each data set, i.e. the model was adjusted to achieve the best results in individual datasets. The practicality of fine-tuning to boost the validation/ out-of-sample data set performance may produce over-fitted models when not combined with ensemble methods. we tried to achieve similar effects by varying the size of fully-convolutional layers and then took the best results.

To compare, we provide the varied architectures by varying the depth size of the transformer branch and the ResNet feature maps.

Table 1: Performance comparison of proposed models with the rest

dataset_name	Existing SOTA	Best:lstm-fcn	Vanilla: ResNet- Transformer	ResNet-Transformer		
				Transformer depth		
				1	4	4
				ResNet feature maps		
				[128, 128, 64, 64]	[128, 128, 64, 64]	[64, 64, 128, 128]
Adiac	0.857	<b>0.869565</b>	0.84399	0.849105	0.849105	0.849105
ArrowHead	0.88	<b>0.925714</b>	0.891429	0.891429	0.891429	0.897143
ChlorineConcentration	<b>0.872</b>	0.816146	0.849479	0.863281	0.409375	0.861719
InsectWingbeatSound	0.6525	<b>0.668687</b>	0.522222	0.642424	0.535859	0.536364
Lightning7	0.863	<b>0.863014</b>	0.821918	0.849315	0.383562	0.835616
Wine	0.889	0.833333	0.851852	0.87037	0.87037	<b>0.907407</b>
WordSynonyms	<b>0.779</b>	0.680251	0.661442	0.65047	0.636364	0.678683
Beef	<b>0.9</b>	<b>0.9</b>	0.866667	0.866667	0.866667	0.866667
DistalPhalanxOutlineAgeGroup	<b>0.835</b>	0.791367	0.81295	0.776978	0.467626	0.776978
DistalPhalanxOutlineCorrect	0.82	0.797101	<b>0.822464</b>	<b>0.822464</b>	<b>0.822464</b>	0.793478
DistalPhalanxTW	<b>0.79</b>	0.748201	0.733813	0.748201	0.719424	0.741007
ECG200	0.92	0.91	0.94	<b>0.95</b>	0.94	0.93
ECGFiveDays	<b>1</b>	0.987224	<b>1</b>	<b>1</b>	<b>1</b>	<b>1</b>
BeetleFly	0.95	<b>1</b>	<b>1</b>	0.95	0.95	<b>1</b>
BirdChicken	0.95	0.95	<b>1</b>	0.9	<b>1</b>	0.7
ItalyPowerDemand	0.97	0.963071	0.965015	0.969874	0.962099	<b>0.971817</b>
SonyAIBORobotSurface1	0.985	0.985025	<b>0.988353</b>	0.978369	0.708819	0.985025
SonyAIBORobotSurface2	0.962	0.972718	0.976915	0.974816	<b>0.98426</b>	0.976915
MiddlePhalanxOutlineAgeGroup	<b>0.8144</b>	0.668831	0.655844	0.662338	0.623377	0.662338
MiddlePhalanxOutlineCorrect	0.8076	0.841924	<b>0.848797</b>	<b>0.848797</b>	<b>0.848797</b>	0.835052
MiddlePhalanxTW	0.612	0.603896	0.564935	0.577922	0.551948	<b>0.623377</b>
ProximalPhalanxOutlineAgeGroup	0.8832	0.887805	0.887805	<b>0.892683</b>	0.882927	<b>0.892683</b>
ProximalPhalanxOutlineCorrect	0.918	<b>0.931271</b>	<b>0.931271</b>	<b>0.931271</b>	0.683849	0.924399

continued on next page

continued from previous page

dataset_name	Existing SOTA	Best:lstm-fcn	Best: ResNet- Transformer	ResNet-Transformer		
				Transformer depth		
				1	4	4
				ResNet feature maps		
				[128, 128, 64, 64]	[128, 128, 64, 64]	[64, 64, 128, 128]
ProximalPhalanxTW	0.815	<b>0.843902</b>	0.819512	0.814634	0.819512	0.819512
MoteStrain	<b>0.95</b>	0.938498	0.940895	0.916933	0.9377	0.679712
MedicalImages	0.792	<b>0.798684</b>	0.780263	0.765789	0.759211	0.789474
Strawberry	0.976	<b>0.986486</b>	<b>0.986486</b>	<b>0.986486</b>	<b>0.986486</b>	<b>0.986486</b>
ToeSegmentationI	0.9737	<b>0.991228</b>	0.969298	0.969298	0.97807	<b>0.991228</b>
Coffee	<b>1</b>	<b>1</b>	<b>1</b>	<b>1</b>	<b>1</b>	<b>1</b>
CricketX	0.821	0.792308	<b>0.838462</b>	0.8	0.810256	0.8
CricketY	0.8256	0.802564	<b>0.838462</b>	0.820513	0.825641	0.807692
CricketZ	0.8154	0.807692	<b>0.820513</b>	0.805128	0.128205	0.1
UWaveGestureLibraryX	0.8308	<b>0.843663</b>	0.780849	0.814629	0.810999	0.808766
UWaveGestureLibraryY	0.7585	<b>0.765215</b>	0.664992	0.71636	0.671413	0.67895
UWaveGestureLibraryZ	0.7725	<b>0.795924</b>	0.756002	0.761027	0.760469	0.762144
ToeSegmentation2	0.9615	0.930769	<b>0.976923</b>	0.953846	0.953846	<b>0.976923</b>
DiatomSizeReduction	0.967	0.970588	0.993464	<b>0.996732</b>	0.379085	<b>0.996732</b>
car	0.933	<b>0.966667</b>	0.95	0.883333	0.866667	0.3
CBF	<b>1</b>	0.996667	<b>1</b>	0.997778	<b>1</b>	<b>1</b>
CinCECGTorso	<b>0.9949</b>	0.904348	0.871739	0.656522	0.89058	0.31087
Computers	0.848	0.852	0.86	0.844	<b>0.908</b>	0.84
Earthquakes	0.801	<b>0.81295</b>	0.755396	0.755396	0.76259	0.755396
ECG5000	0.9482	<b>0.948222</b>	0.941556	0.943556	0.944222	0.940444
ElectricDevices	<b>0.7993</b>	0.779665	0.774219	0.771625	0.757489	0.766178
FaceAll	0.929	<b>0.956213</b>	0.881065	0.848521	0.949704	0.252071
FaceFour	<b>1</b>	0.943182	0.954545	0.965909	0.977273	0.215909
FacesUCR	<b>0.958</b>	0.941463	0.957561	0.947805	0.926829	0.95122
Fish	0.989	0.971429	<b>1</b>	0.977143	0.96	0.994286
FordA	0.9727	<b>0.976515</b>	0.948485	0.946212	0.517424	0.940909
FordB	<b>0.9173</b>	0.792593	0.838272	0.830864	0.838272	0.823457
GunPoint	<b>1</b>	<b>1</b>	<b>1</b>	<b>1</b>	<b>1</b>	<b>1</b>
Ham	0.781	<b>0.809524</b>	0.761905	0.780952	0.619048	0.514286
HandOutlines	0.9487	<b>0.954054</b>	0.937838	0.948649	0.835135	0.945946
Haptics	0.551	0.558442	0.564935	0.545455	<b>0.600649</b>	0.194805
Herring	0.703	<b>0.75</b>	0.703125	0.734375	0.65625	0.703125
InlineSkate	<b>0.6127</b>	0.489091	0.516364	0.494545	0.494545	0.165455
LargeKitchenAppliances	0.896	0.898667	0.928	0.898667	<b>0.936</b>	0.933333
Lighting2	<b>0.8853</b>	0.819672	0.852459	0.852459	0.754098	0.868852
MALLAT	0.98	<b>0.98081</b>	0.977399	0.975267	0.934328	0.979104
Meat	<b>1</b>	0.883333	<b>1</b>	<b>1</b>	<b>1</b>	<b>1</b>
NonInvasiveFetalECGThorax1	0.961	<b>0.970483</b>	0.953181	0.953181	0.947583	0.948092
NonInvasiveFetalECGThorax2	0.955	<b>0.961323</b>	0.955216	0.954198	0.948601	0.952672
OliveOil	0.9333	0.766667	<b>0.966667</b>	0.9	0.933333	0.9
OSULeaf	0.988	0.983471	0.987603	<b>0.991736</b>	0.987603	<b>0.991736</b>
PhalangesOutlinesCorrect	0.83	0.83683	<b>0.855478</b>	0.848485	0.854312	0.850816
Phoneme	0.3492	0.341772	<b>0.363924</b>	0.191983	0.357595	0.348101
plane	<b>1</b>	<b>1</b>	<b>1</b>	<b>1</b>	0.371429	<b>1</b>
RefrigerationDevices	0.5813	0.605333	0.605333	0.616	0.592	<b>0.618667</b>
ScreenType	<b>0.707</b>	0.682667	0.669333	0.645333	0.666667	0.68
ShapeletSim	<b>1</b>	<b>1</b>	<b>1</b>	0.911111	0.888889	0.977778
ShapesAll	0.9183	0.905	0.923333	0.876667	0.921667	<b>0.933333</b>
SmallKitchenAppliances	0.803	0.821333	0.808	0.810667	<b>0.829333</b>	0.813333
StarlightCurves	0.9796	0.977295	<b>0.978873</b>	0.979237	<b>0.978873</b>	0.975838
SwedishLeaf	0.9664	<b>0.9792</b>	<b>0.9792</b>	0.9728	0.9696	0.9664
Symbols	0.9668	<b>0.98794</b>	0.9799	0.970854	0.976884	0.252261
SyntheticControl	<b>1</b>	0.993333	<b>1</b>	0.996667	<b>1</b>	<b>1</b>
Trace	<b>1</b>	<b>1</b>	<b>1</b>	<b>1</b>	<b>1</b>	<b>1</b>
TwoPatterns	<b>1</b>	0.99675	<b>1</b>	<b>1</b>	<b>1</b>	<b>1</b>
TwoLeadECG	<b>1</b>	<b>1</b>	<b>1</b>	<b>1</b>	<b>1</b>	<b>1</b>

continued on next page

continued from previous page

dataset_name	Existing SOTA	Best:lstm-fcn	Best: ResNet- Transformer	ResNet-Transformer		
				Transformer depth		
				1	4	4
				ResNet feature maps		
				[128, 128, 64, 64]	[128, 128, 64, 64]	[64, 64, 128, 128]
UWaveGestureLibraryAll	<b>0.9685</b>	0.961195	0.856784	0.933277	0.939978	0.879118
wafer	<b>1</b>	0.998378	0.99854	0.998215	0.99854	0.999027
Worms	0.8052	<b>0.844156</b>	0.831169	0.779221	0.818182	0.25974
WormsTwoClass	0.8312	0.844156	<b>0.857143</b>	0.831169	0.805195	0.831169
yoga	0.9183	<b>0.921667</b>	0.906333	0.905667	0.884	0.866667
ACSF1	-	0.9	<b>0.96</b>	0.91	0.93	0.17
AllGestureWiimoteX	-	0.701429	0.77	0.76	<b>0.762857</b>	0.754286
AllGestureWiimoteY	-	0.802857	<b>0.814286</b>	0.798571	0.808571	0.8
AllGestureWiimoteZ	-	0.684286	<b>0.782857</b>	0.752857	0.767143	0.748571
BME	-	0.993333	<b>1</b>	<b>1</b>	<b>1</b>	<b>1</b>
Chinatown	-	0.982609	<b>0.985507</b>	<b>0.985507</b>	<b>0.985507</b>	<b>0.985507</b>
Crop	-	0.74494	0.743869	0.742738	<b>0.746012</b>	0.740476
DodgerLoopDay	-	<b>0.6375</b>	0.5375	0.55	0.4625	0.5
DodgerLoopGame	-	0.898551	0.876812	0.891304	0.550725	<b>0.905797</b>
DodgerLoopWeekend	-	<b>0.978261</b>	0.963768	0.978261	0.949275	0.963768
EOGHorizontalSignal	-	<b>0.654696</b>	0.610497	0.59116	0.60221	0.610497
EOGVerticalSignal	-	<b>0.505525</b>	0.450276	0.48895	0.146409	0.480663
EthanolLevel	-	0.772	0.824	<b>0.868</b>	0.82	0.802
FreezerRegularTrain	-	0.997895	<b>0.999649</b>	0.999298	0.999298	<b>0.999649</b>
FreezerSmallTrain	-	0.825965	<b>0.975088</b>	0.958947	0.906667	0.771579
Fungi	-	0.994624	<b>1</b>	<b>1</b>	0.994624	0.075269
GestureMidAirD1	-	0.715385	0.715385	<b>0.723077</b>	<b>0.723077</b>	0.7
GestureMidAirD2	-	0.707692	<b>0.746154</b>	0.692308	0.676923	0.7
GestureMidAirD3	-	<b>0.430769</b>	0.353846	0.369231	0.338462	0.338462
GesturePebbleZ1	-	0.918605	<b>0.936047</b>	0.831395	<b>0.936047</b>	0.906977
GesturePebbleZ2	-	0.886076	0.873418	0.841772	<b>0.911392</b>	0.879747
GunPointAgeSpan	-	0.996835	0.996835	0.996835	<b>1</b>	0.848101
GunPointMaleVersusFemale	-	<b>1</b>	<b>1</b>	<b>1</b>	0.996835	0.996835
GunPointOldVersusYoung	-	0.993651	<b>1</b>	<b>1</b>	<b>1</b>	0.990476
HouseTwenty	-	0.983193	0.983193	0.907563	0.983193	<b>0.991597</b>
InsectEPGRegularTrain	-	0.995984	<b>1</b>	<b>1</b>	<b>1</b>	<b>1</b>
InsectEPGSmallTrain	-	0.935743	0.955823	0.927711	<b>0.971888</b>	0.477912
MelbournePedestrian	-	<b>0.913061</b>	0.912245	0.911837	0.904898	0.901633
MixedShapesRegularTrain	-	0.973608	0.97567	0.969897	0.97567	<b>0.980206</b>
MixedShapesSmallTrain	-	0.936082	0.910103	0.918763	0.92866	<b>0.940619</b>
PickupGestureWiimoteZ	-	0.74	<b>0.8</b>	0.78	0.78	0.78
PigAirwayPressure	-	<b>0.336538</b>	<b>0.336538</b>	0.096154	0.173077	0.153846
PigArtPressure	-	<b>1</b>	<b>1</b>	0.168269	0.043269	0.533654
PigCVP	-	0.875	<b>0.908654</b>	0.081731	0.211538	0.019231
PLAID	-	0.901304	0.944134	0.921788	0.147114	<b>0.945996</b>
PowerCons	-	<b>0.994444</b>	0.933333	0.944444	0.927778	0.927778
Rock	-	<b>0.92</b>	0.78	<b>0.92</b>	0.82	0.76
SemgHandGenderCh2	-	0.91	0.866667	<b>0.916667</b>	0.848333	0.651667
SemgHandMovementCh2	-	<b>0.56</b>	0.513333	0.504444	0.391111	0.468889
SemgHandSubjectCh2	-	<b>0.873333</b>	0.746667	0.74	0.666667	0.788889
ShakeGestureWiimoteZ	-	0.88	<b>0.94</b>	<b>0.94</b>	<b>0.94</b>	<b>0.94</b>
SmoothSubspace	-	0.98	<b>1</b>	<b>1</b>	0.993333	<b>1</b>
UMD	-	0.986111	<b>1</b>	<b>1</b>	<b>1</b>	<b>1</b>

## 4 Conclusion

We present RAN as a potential new architecture for time-series or sequence-driven modeling. Out of the standard 85 UCR data sets, we have achieved 35 state-of-the-art results with 10 results matching current state-of-the-art results without further model fine-tuning. The results indicate that such

Table 2: Wilcoxon signed rank test comparison of each model

	resnet-transformer	lstm-fcn	tfcn	Resnet	fcn	1-NN DTW CV	1-NN DTW	BOSS	Learning Shapelet (LS)	TSBF	ST	EE (PROP)	COTE (ensemble)	MLP	CNN
lstm-fcn	0.096581	0													
tfcn	3.76E-06	5.30E-06	0												
Resnet	1.03E-08	1.82E-06	0.005163	0											
fcn	2.92E-11	1.45E-08	0.001401	0.958291	0										
1-NN DTW CV	1.52E-13	3.48E-13	5.74E-12	3.69E-10	1.53E-07	0									
1-NN DTW	2.81E-14	4.45E-14	5.64E-13	8.44E-13	2.98E-10	0.000381	0								
BOSS	1.79E-12	1.43E-10	2.52E-06	0.002485	0.012174	2.67E-07	1.11E-10	0							
Learning Shapelet (LS)	7.05E-12	1.65E-11	8.39E-09	9.77E-06	0.000346	0.000416	1.04E-06	0.032497	0						
TSBF	1.49E-12	1.10E-12	1.65E-09	1.70E-08	1.59E-06	0.014259	5.39E-05	0.001402	0.423474	0					
ST	5.02E-11	8.09E-11	5.57E-06	0.006204	0.004078	1.61E-07	5.75E-10	0.15641	0.002506	0.00031	0				
EE (PROP)	1.23E-11	7.22E-11	5.22E-08	1.66E-06	0.000117	8.67E-10	1.71E-11	0.022618	0.935015	0.518861	0.001094	0			
COTE (ensemble)	2.38E-09	2.25E-07	0.002011	0.438745	0.144622	1.82E-13	5.82E-14	0.000584	2.20E-09	8.15E-09	0.001998	1.55E-11	0		
MLP	3.63E-13	4.91E-13	1.56E-12	5.94E-08	9.91E-07	0.924497	0.168452	0.000426	0.017383	0.046248	2.19E-05	0.016323	8.66E-08	0	
CNN	8.40E-09	4.20E-06	0.168655	0.222513	0.316416	9.73E-10	3.14E-12	0.001762	1.18E-06	4.24E-08	0.00088	8.24E-07	0.114445	2.78E-10	0

architecture is promising in complex, long-sequence modeling and may have vast, cross-domain applications.

## References

- [1] Karim Ahmed, Nitish Shirish Keskar, and Richard Socher. Weighted transformer network for machine translation. *arXiv preprint arXiv:1711.02132*, 2017.
- [2] Shaojie Bai, J Zico Kolter, and Vladlen Koltun. An empirical evaluation of generic convolutional and recurrent networks for sequence modeling. *arXiv preprint arXiv:1803.01271*, 2018.
- [3] Yi Bin, Yang Yang, Fumin Shen, Ning Xie, Heng Tao Shen, and Xuelong Li. Describing video with attention-based bidirectional lstm. *IEEE transactions on cybernetics*, 49(7):2631–2641, 2018.
- [4] Mostafa Dehghani, Stephan Gouws, Oriol Vinyals, Jakob Uszkoreit, and Łukasz Kaiser. Universal transformers. *arXiv preprint arXiv:1807.03819*, 2018.
- [5] Jacob Devlin, Ming-Wei Chang, Kenton Lee, and Kristina Toutanova. Bert: Pre-training of deep bidirectional transformers for language understanding. *arXiv preprint arXiv:1810.04805*, 2018.
- [6] H Ismail Fawaz, Germain Forestier, Jonathan Weber, Lhassane Idoumghar, and P Muller. Deep neural network ensembles for time series classification. *arXiv preprint arXiv:1903.06602*, 2019.
- [7] Qipeng Guo, Xipeng Qiu, Pengfei Liu, Yunfan Shao, Xiangyang Xue, and Zheng Zhang. Star-transformer. *arXiv preprint arXiv:1902.09113*, 2019.
- [8] Kaiming He, Xiangyu Zhang, Shaoqing Ren, and Jian Sun. Deep residual learning for image recognition. In *Proceedings of the IEEE conference on computer vision and pattern recognition*, pages 770–778, 2016.
- [9] Fazle Karim, Somshubra Majumdar, and Houshang Darabi. Insights into lstm fully convolutional networks for time series classification. *IEEE Access*, 2019.
- [10] Fazle Karim, Somshubra Majumdar, Houshang Darabi, and Shun Chen. Lstm fully convolutional networks for time series classification. *IEEE Access*, 6:1662–1669, 2017.
- [11] Fazle Karim, Somshubra Majumdar, Houshang Darabi, and Samuel Harford. Multivariate lstm-fcns for time series classification. *Neural Networks*, 116:237–245, 2019.
- [12] Sangyeon Kim and Myungjoo Kang. Financial series prediction using attention lstm. *arXiv preprint arXiv:1902.10877*, 2019.
- [13] Jun Liu, Gang Wang, Ping Hu, Ling-Yu Duan, and Alex C Kot. Global context-aware attention lstm networks for 3d action recognition. In *Proceedings of the IEEE Conference on Computer Vision and Pattern Recognition*, pages 1647–1656, 2017.
- [14] Christopher Martin. Neural network architecture using control logic determining convolution operation sequence, May 16 2019. US Patent App. 16/182,369.
- [15] Matthieu Riou, Bassam Jabaian, Stéphane Huet, and Fabrice Lefèvre. Reinforcement adaptation of an attention-based neural natural language generator for spoken dialogue systems. *Dialogue & Discourse*, 10(1):1–19, 2019.
- [16] Youngjoo Seo, Michaël Defferrard, Pierre Vandergheynst, and Xavier Bresson. Structured sequence modeling with graph convolutional recurrent networks. In *International Conference on Neural Information Processing*, pages 362–373. Springer, 2018.
- [17] Ahmed Shifaz, Charlotte Pelletier, Francois Petitjean, and Geoffrey I Webb. Ts-chief: A scalable and accurate forest algorithm for time series classification. *arXiv preprint arXiv:1906.10329*, 2019.
- [18] Huan Song, Deepta Rajan, Jayaraman J Thiagarajan, and Andreas Spanias. Attend and diagnose: Clinical time series analysis using attention models. In *Thirty-Second AAAI Conference on Artificial Intelligence*, 2018.
- [19] Ashish Vaswani, Noam Shazeer, Niki Parmar, Jakob Uszkoreit, Llion Jones, Aidan N Gomez, Łukasz Kaiser, and Illia Polosukhin. Attention is all you need. In *Advances in neural information processing systems*, pages 5998–6008, 2017.
- [20] Bo Zeng, Dongbo Zhao, Chanan Singh, Jianhui Wang, and Chen Chen. Holistic modeling framework of demand response considering multi-timescale uncertainties for capacity value estimation. *Applied Energy*, 247:692–702, 2019.

- [21] Kuangen Zhang, Ming Hao, Jing Wang, Clarence W de Silva, and Chenglong Fu. Linked dynamic graph cnn: Learning on point cloud via linking hierarchical features. *arXiv preprint arXiv:1904.10014*, 2019.
- [22] Yongbing Zhang, Tao Shen, Xiangyang Ji, Yun Zhang, Ruiqin Xiong, and Qionghai Dai. Residual highway convolutional neural networks for in-loop filtering in hevcc. *IEEE Transactions on Image Processing*, 27(8):3827–3841, 2018.